

Modelling kinematics and cutting forces in vibration assisted drilling

JOHN LE DREF^{1,a}, YANN LANDON², GILLES DESSEIN¹ AND CHRISTINE ESPINOSA²

¹ Laboratoire Génie de Production, École Nationale d'Ingénieurs de Tarbes, 65016 Tarbes, France

² Institut Clément Ader (ICA) Université de Toulouse, INSA, UPS, Mines Albi, 31062 Toulouse, France

Received 12 November 2014, Accepted 28 September 2015

Abstract – One of the main drawbacks of the traditional drilling process is the formation of long chips when cutting metallic parts. Usually, peck drilling cycles are used to break and evacuate the chips through the flutes of the drill. However, this solution increases the operation time and therefore decreases the productivity. To solve this problem, vibration assisted drilling has been developed to meet industrial needs in terms of productivity. Forced vibrations impose a variation of the chip thickness in order to obtain its fragmentation. This process has been recently developed and optimal cutting conditions have yet to be determined to improve it furthermore. This paper presents, on the first hand, an experimental study of the kinematics of vibration assisted drilling. It showed a strong reduction of the amplitude of vibration during drilling, in the configuration of the tests. In addition, tests were conducted to show the apparition of interference phenomena at the centre of the tool. Interferences are difficult to separate from the cutting phenomenon, making the modelling of cutting forces difficult. From the kinematic model, chip height can be simulated in order to model the cutting forces. A thrust force and a torque model applied to vibration assisted drilling are presented in this paper. The thrust force model is based on a representation of the tool by several zones corresponding to each cutting mechanism: indentation at the centre of the tool, cutting along the cutting edges and bad cutting conditions in an intermediary zone. The periodically variable feed speed modifies the size of each zone and the thrust force they generate. The model presented in this paper formulates the interaction of several zones of the tool with the material and explains the particular shape of the thrust force observed. The models are identified and validated through an application on aluminium alloy 7010.

Key words: Vibration assisted drilling / thrust force / torque / kinematic model

1 Introduction

When drilling metallic parts, long chips are often generated. Deburring cycles can be used to fragment the chips and to evacuate them through the flutes of the drill. However, by including deburring cycles, productivity is decreased. Another alternative is to enforce their breaking. The principle of vibration assisted drilling is the addition of oscillations to the traditional feed movement. Oscillations are thus added to the constant feed of the tool. The chip height becomes variable and low enough to force a fragmentation of chips, depending on the material to be cut.

Several solutions to generate vibrations during the drilling operation exist. For the first type of vibration assistance, chatter vibrations are generated with specific

cutting parameters [1]. A complex dynamic study is necessary to determine the optimal parameters. Else, vibrations can be forced, hence with specific frequencies and amplitudes. For instance, piezoelectric devices generate high frequencies and low amplitudes vibrations [2].

Another possibility is the use of a mechanical system [3]. In this study, the tool holder MITIS PG 80–40 is equipped with a mechanical cam. The system consists in a low frequency and high amplitude forced vibration device. It generates 1.5 oscillations per revolution of the tool. The amplitude is adjustable on this specific tool-holder, from 0 to 0.5 mm.

The use of oscillations along the axis of the tool ensures chip fragmentation in metals if the amplitude is important enough in regard to the feed. It then permits an easier chip removal from the cutting area [4, 5]. However, its impact on the hole quality is undetermined as well as the changes that tool vibrations cause to the cutting

^a Corresponding author: john.ledref@gmail.com

mechanisms. Burrs on metals [6,7], delamination and surface quality on composites [8–10] are considered the most important defects in drilling. The impact of vibrations on those defects has to be studied. For this task, the definition of the kinematics of the process, as well as the modelling of cutting forces, are necessary. The kinematic model permits the determination of the chip height and of the feed rate at any instant of the cutting operation. These parameters can then be used in the prediction of thrust force and torque.

The model of the thrust force in vibration assisted drilling suggested is based on the model presented in the work of Guibert et al. [11]. In this model, the drill is represented by several zones corresponding to specific mechanisms. This model is adapted to vibration drilling to take into account the important variations of the two parameters, chip height and the instantaneous feed rates, in vibration assisted drilling. The size of each zone and the force they generate depend on those two parameters.

Previous studies determined the chip height from the kinematic model [4] by defining the trajectory of any point of the tool in vibration assisted drilling. However, differences between the experimental kinematic of the process and the simulation were pointed out. It is therefore difficult to simulate a chip height and a thrust force model depending on the theoretical trajectories without correcting the real kinematic behaviour of the system.

This paper presents a study of the kinematics and the cutting forces generated in vibration assisted drilling. In a first part, the kinematic of the process is modelled. Moreover, a thrust force model and a torque model applied to vibrations assisted drilling are suggested. The coefficients of the thrust force model are identified through experiments on traditional drilling of aluminum alloy 7010. The thrust force model is adapted to vibration assisted drilling. It explains the particular evolution of the thrust force related to the important variation of the instantaneous feed rate induced by the oscillations.

The comparison between force measurements and simulations shows that the kinematic model is not accurate enough. Then, a corrected kinematic model is suggested in order to take into account the phenomenon specific to vibration assisted drilling, and which explains the differences observed between the kinematic model and the experimental data. The reduction of amplitude of the vibrations during drilling will be assessed and taken into account. The differences in cutting time are also explained by the presence of interferences at the centre of the tool.

2 Modelling of the vibration assisted drilling

2.1 Study of the kinematics in vibration assisted drilling

Before modelling the thrust force in vibration assisted drilling, it is necessary to determine the chip height by establishing a kinematic model of the process, based on the previous work of Jallageas [4]. The trajectory of any point of the tool is defined with a constant feed movement

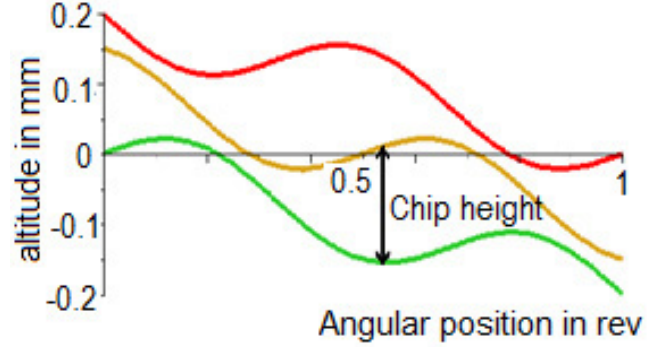


Fig. 1. Representation of tool trajectories and chip height in the case of continuous cutting.

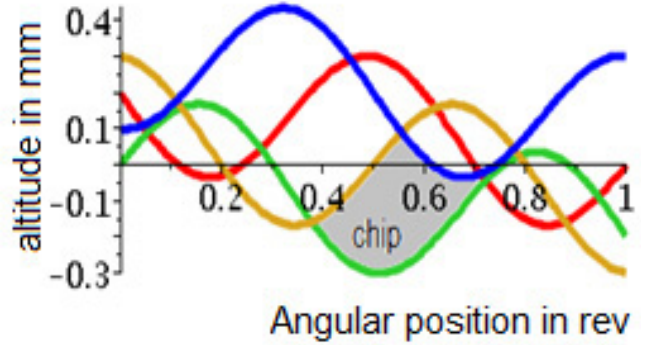


Fig. 2. Representation of tool trajectories and chip height in the case of interrupted cutting.

and the added oscillations. It is convenient to express the altitude of a point of the edge of the tool as a function of the angular position. The angular position w is expressed in revolutions. The formula of the trajectory $Z_i(w)$ of the i -th tooth is as follows (Eq. (1)):

$$Z_i(w) = -fw + \frac{a}{2} \sin \left(Osc 2\pi w - \frac{i}{Z} 2\pi Osc \right) + i \frac{f}{Z} \quad (1)$$

where f is the feed in $\text{mm}\cdot\text{rev}^{-1}$, a the amplitude of oscillations, Osc the frequency of oscillations in $\text{osc}\cdot\text{rev}^{-1}$, Z number of teeth of the tool, w the angular position in rev.

The chip height at any given angular position can be defined from these tool trajectories by calculating the difference between the current trajectory and the previous ones (Fig. 1 and Eq. (2))

$$Z_{i+1}(w) - Z_i(w) = \frac{f}{Z} + \frac{a}{2} \left[2 \sin \left(-\frac{\pi Osc}{Z} \right) \times \cos \left(2\pi Osc w - \frac{\pi Osc}{Z} \right) \right] \quad (2)$$

When the amplitude is important enough for a given feed, several trajectories can intersect. In this case, it is necessary to define the surface left by the previous tooth passage to simulate the chip height (Fig. 2).

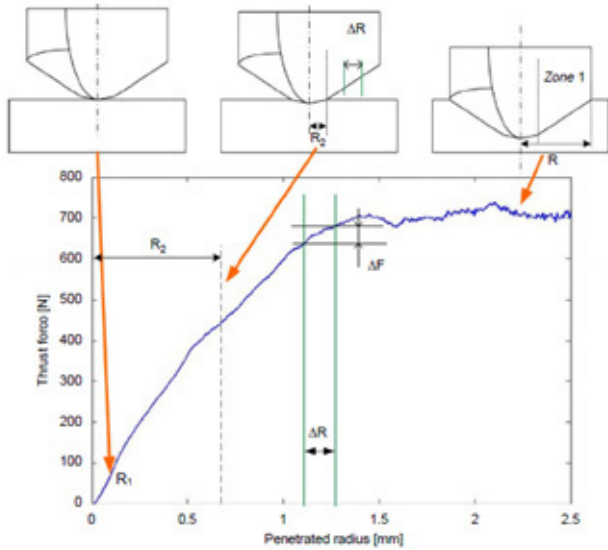


Fig. 3. Thrust force measured as a function of penetrated radius and observation of the changes of slope [11].

The limit between continuous and interrupted cutting corresponds to the case where two consecutive trajectories are tangent. In this special case, the amplitude (noted a_f) can be expressed in relation to the feed f , the frequency Osc and the number of teeth Z (Eq. (3))

$$a_f = \frac{f}{Z \sin\left(\frac{\pi Osc}{Z}\right)} \quad (3)$$

If the amplitude is set below this limit, the cutting is continuous. If the amplitude is set over this limit, the cutting will be interrupted as teeth trajectories intersect previous ones

2.2 Thrust force and torque modelling

The thrust force model presented in this paper is based on the model established by Guibert et al. [11], modified to take into account the forced vibration and its consequences. The identification of the coefficients of the model follows the edge-material pair method in traditional drilling: for the entry of the tool-tip, the thrust force versus time (or penetrated radius) is plotted, considering perfect tool geometry. Changes of slope on the thrust force signal point out different cutting mechanisms. Three of them are identified (Fig. 3).

These three zones are explained by the combination of the local geometry of the tool and the local kinematics (Fig. 4). They are determined by the study of the force signal and its derivative at the entry of the tip of the tool.

- At the centre of the tool, there is a close to null cutting speed. This part of the tool works as an indenter, pushing out the material, generating a large amount of thrust force in comparison to its size.
- Farther from the centre, on an intermediary zone, the cutting speed is important enough to have a cutting

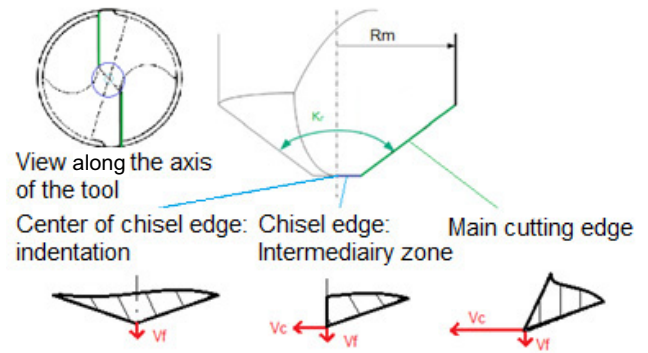


Fig. 4. Main cutting phenomena in drilling operation.

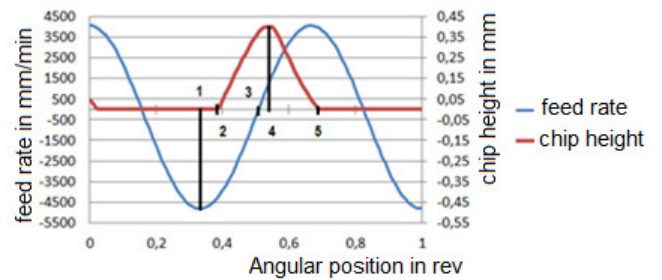


Fig. 5. Phase-shifted feed rate and chip height for $f = 0.2 \text{ mm}\cdot\text{rev}^{-1}$ and $a = 0.32 \text{ mm}$.

phenomenon, but not enough for the cutting phenomenon to be efficient. The part of the total force generated by this zone increases rapidly with the feed, up to 40% of the total thrust force for feed rates higher than $0.2 \text{ mm}\cdot\text{rev}^{-1}$ in drilling steel 35MnV7 with a 5 mm diameter carbide drill [11].

- On the cutting edges, the cutting speed increases with the radius and it is several times the value of the feed rate. Because the feed rate is negligible in front of the cutting speed on the main edges of the tool, the thrust force generated is mainly related to the chip height.

As far as traditional drilling is concerned, chip height and feed rate are constant: therefore cutting mechanism and its associated area are also constant. When considering vibration assisted drilling, chip height and feed rate are varying with time. Moreover, the correlation between those two through the rotational speed is irrelevant (Fig. 5).

An example of the evolution of the chip height and the instantaneous feed rate are shown in Figure 5. It can be seen that the tool enters the material (2) when the feed rate is close to its maximum in absolute value (1) and the tool goes downward ($V_{fi} < 0$). Then, the chip height gets to its maximum value (4) when the feed rate is close to zero (3). Finally, the tooth exits the material (5) when the tool goes upward ($V_{fi} > 0$).

Interactions between the chip height and the instantaneous feed rate V_{fi} are expected, in regards to the size of each zone and the thrust force generated for each mechanism encountered. In contrary to the cutting edges where the cutting speed is high, the indentation zone and the

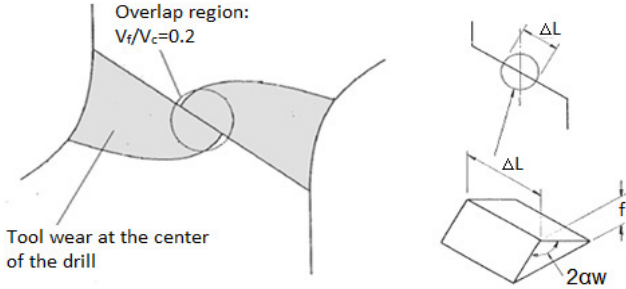


Fig. 6. Tool wear and approximate indentation radius.

intermediary zone are highly related to the feed rate. The extents of their areas as well as the thrust force generated may both be increasing with the feed rate in vibration assisted drilling. It calls for changes on the thrust force models of those two zones.

Because the feed rate varies, and bears both positive and negative values, a few assumptions were made:

- When the instantaneous feed rate is positive (the tool goes up) there is no indentation. It becomes part of the ploughing zone which presents bad cutting conditions.
- The indentation zone has its area related to the feed rate. The chip height regulates the size of the other zones since the higher cutting speed implies cutting mechanisms and chipping.

The size of each zone and the models of thrust force F_z associated are determined with traditional drilling data. Their formulas are presented in the next part.

The model presented in this paper is compared to a power regression model (Eq. (4)), also identified with traditional drilling data:

$$F_z = K_p \Delta R h_c^{q_p} \quad (4)$$

where ΔR is the tool radius, h_c the chip height, K_p and q_p to be determined.

2.2.1 Indentation zone

In reference [12], a theoretical radius is calculated for the indentation zone (Fig. 6). The radius corresponds to the point for which the cutting speed is 5 times the feed rate. It accounts for a few tenths of mm. However, this model is arbitrary and empirical as it is defined on wear observation on the tip of the tool.

Reference [11] suggested an experimental definition of the indentation radius in function of the feed: by deriving the thrust force, it is possible to point out precisely the first change of slope corresponding to the indentation phenomenon.

In this paper, the indentation radius ΔR_{ind} is chosen to be represented as a function of the feed rate V_f instead of the feed f (Eq. (5)).

A fractional model [13] is used to model the indentation force F_{ind} (Eq. (6)). The indentation radius ΔR_{ind}

and the indentation force are identified through experimental data from traditional drilling tests.

$$\Delta R_{ind} = K_{rind} V_f^{q_{rind}} \quad (5)$$

where K_{rind} and q_{rind} are parameters.

$$F_{ind} = K_{ind} h_c^* \Delta R_{ind} \frac{\left(\frac{h_c}{h_c^*}\right) + r_c \left(\frac{h_c}{h_c^*}\right)^2}{1 + \left(\frac{h_c}{h_c^*}\right)} \quad (6)$$

where h_c is the chip height, ΔR_{ind} the indentation radius previously measured and modeled, h_c^* and K_{ind} parameters.

It is assumed that, when the feed rate is positive and the tool goes upward, the extent of the indentation zone is zero: there is no indentation when the tool goes up. However, the tool is still locally in contact with the material, meaning that the area induces another cutting mechanism: it is swept into the intermediary area.

2.2.2 Intermediary zone

In the second zone, chips are generated but the cutting speeds are not important enough. Moreover, this intermediary zone has to cut additional material which was indented and displaced by the first zone.

The extent of the zone ΔR_{pe} is determined by the observation of the thrust force measured at the entry of the tip of the tool for different feed. It is modelled by the following equation, as a function of chip height (Eq. (7)).

$$\Delta R_{pe} = K_{rpe} h_c^{r_{pe}} + r_0 \quad (7)$$

where K_{rpe} , r_{pe} , r_0 are parameters.

The force F_{pe} generated by this zone is modelled with (Eq. (8)) as a function of this radius and the chip height:

$$F_{pe} = K_{pe} (1 - \sin \gamma_{fe})^{q_{pe}} \Delta R_{pe} h_c^{d_{pe}} \quad (8)$$

where the parameters to identify are K_{pe} , q_{pe} , d_{pe} , γ_{fe} the cutting rake angle in $^\circ$, and h_c the chip height.

The influence of the feed rate on the thrust force generated is taken into account through the instantaneous dynamic rake angle γ_{fe} . The force generated by the intermediary zone is increased when the feed rate is negative, i.e. the tool goes downward.

2.2.3 Main cutting zone

In the cutting zone, the cutting speed ranges approximately from 10% to 100% of its maximum value at the diameter of the tool. Because the cutting speed V_c at any given radius of the cutting zone is high, the influence of the feed rate is reduced but still considered. The variation of the instantaneous feed rate in vibration assisted drilling implies a feeble variation of the dynamic rake angle. The important variation of the cutting speed V_c has a greater influence on the thrust force. As the cutting

speed increases with the radius, it is expected that the mean cutting pressure lowers and the thrust force is reduced. The model, presented in [11] for the cutting zone, is unaltered. It calculates the thrust force locally for each element with a length ΔR_c (Eq. (9)) and sums them up to get the total contribution of the cutting edges (Eq. (10)). It makes it possible to define the influence of the variation of both cutting speed and feed rate in vibration assisted drilling as they appear in the calculation of the dynamic rake angle.

$$\Delta F_c = K_c (1 - \sin \gamma_{fe})^{q_c} V_c^b \Delta R_c h_c^{d_c} \quad (9)$$

$$F_c = \sum_i \Delta F_{ci} \quad (10)$$

where K_c , q_c , b and d_c are identified with traditional drilling data, γ_{fe} the mean rake angle at the element concerned, V_c its velocity.

3 Experimental procedures

The drilling tests were carried out on a five-axis CNC machining centre, with two different twist drills: drill 1 $\text{Ø}12.7$ mm and drill 2 $\text{Ø}15.9$ mm, with two lips and a drill point thinning. Internal minimal quantity lubrication was used. Cutting forces were measured using a Kistler 9257B dynamometer. Aluminum alloy 7010 was drilled at several feeds, from $0.025 \text{ mm} \cdot \text{rev}^{-1}$ to $1 \text{ mm} \cdot \text{rev}^{-1}$, and with a cutting speed of $75 \text{ m} \cdot \text{min}^{-1}$ in traditional drilling. For feed higher than $0.3 \text{ mm} \cdot \text{rev}^{-1}$, only the tip of the tool penetrated the material to avoid unnecessary tool wear or tool breakage. The simulation obtained through traditional drilling data is verified with vibration assisted drilling tests for two values of feed ($0.1 \text{ mm} \cdot \text{rev}^{-1}$; $0.2 \text{ mm} \cdot \text{rev}^{-1}$) and several amplitudes of vibrations a from 0.05 mm to 0.5 mm. The shape of chip was controlled for each test.

In addition, drilling tests were carried out on rods and on pilot holes. The aim of those tests is to highlight the different mechanisms generated in the centre of the tool and by the cutting edges. The evolutions of the chip height and of the thrust force measured during vibration assisted drilling are also analysed. For these tests on rods and pilot holes, the twist drill 1 $\text{Ø}12.7$ mm was used, with a feed of $0.2 \text{ mm} \cdot \text{rev}^{-1}$ and a cutting speed of $75 \text{ m} \cdot \text{min}^{-1}$. Rods and pilot holes of $\text{Ø}2.7$ mm and $\text{Ø}4.14$ mm are prepared on the aluminum alloy 7010 plate (Fig. 7). Several amplitudes of oscillations a from 0 mm to 0.5 mm are tested.

4 Results and discussions

4.1 Thrust force model

Using the edge-material pair method, developed by Bissey-Breton and quoted in the work of Guibert et al. [11], the parameters of the model suggested are determined from traditional drilling data. The size of each

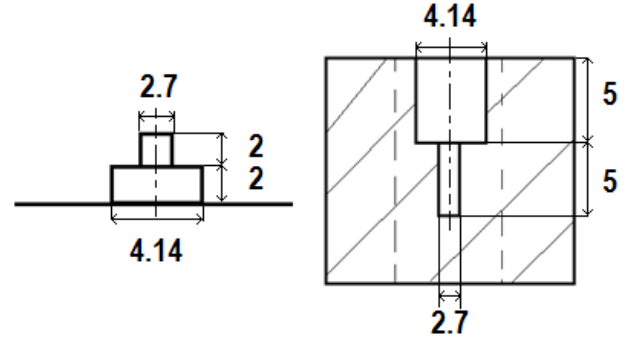


Fig. 7. Rods and pilot holes prepared on AA7010 plate.

zone is identified by observing the changes of slope on the thrust force signal. The thrust forces each zone generates are then measured, allowing the identification of all the parameters.

Concerning the power model (Eq. (4)), it is identified as a function of the chip height by observing the total thrust force generated for each feed rate studied.

The results of the two studies are given below:

– Power model

$$K_p = 331.91, \quad q_p = 0.52, \quad R^2 > 0.98$$

– Indentation zone

$$K_{\text{rind}} = 0.011, \quad q_{\text{rind}} = 0.571, \quad R^2 = 0.94$$

$$K_{\text{ind}} = 6426.30, \quad h_c^* = 0.003, \quad r_c = 0.253, \quad R^2 = 0.56$$

– Intermediary zone

$$K_{\text{rpe}} = 5.704, \quad q_{\text{rpe}} = 0.702, \quad R^2 = 0.97$$

$$K_{\text{pe}} = 405.41, \quad q_{\text{pe}} = 0.49, \quad d_{\text{pe}} = -2.53, \quad R^2 > 0.95$$

– Cutting zone

$$K_c = 6196.84, \quad q_c = 0.36, \quad b = 1.04, \\ d_c = -0.107, \quad R^2 > 0.98$$

Several comparisons of the model and the power regression model with experimental data in vibration assisted drilling are represented over one revolution of the tool (Figs. 8–10).

At low amplitude of vibrations (Fig. 8), it can be seen that the thrust force measured is close to a sinusoid as is the theoretical chip height. However, when the amplitude is increased, a particular shape of the thrust force can be seen (Figs. 9 and 10). The first part, in regards to the tool going down, shows a fast increase of the thrust force. On the second part, as the tool goes upward, the shape of the thrust force shows successive changes. In contrary to the power model, the model suggested points out this behaviour in vibration assisted drilling, which is a direct consequence of the separate modelling of each cutting mechanism.

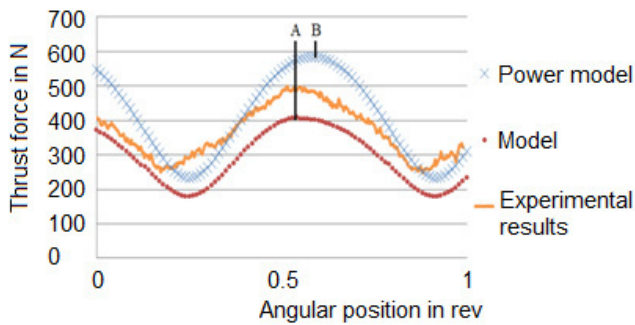


Fig. 8. Comparison of experimental and theoretical thrust forces for $f = 0.1 \text{ mm}\cdot\text{rev}^{-1}$ and $a = 0.05 \text{ mm}$.

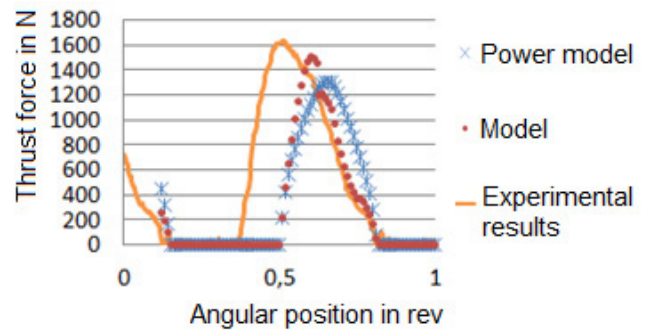


Fig. 10. Comparison of experimental and theoretical thrust forces for $f = 0.2 \text{ mm}\cdot\text{rev}^{-1}$ and $a = 0.5 \text{ mm}$.

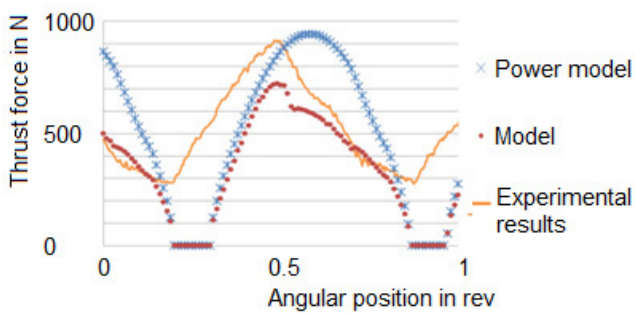


Fig. 9. Comparison of experimental and theoretical thrust forces for $f = 0.2 \text{ mm}\cdot\text{rev}^{-1}$ and $a = 0.16 \text{ mm}$.

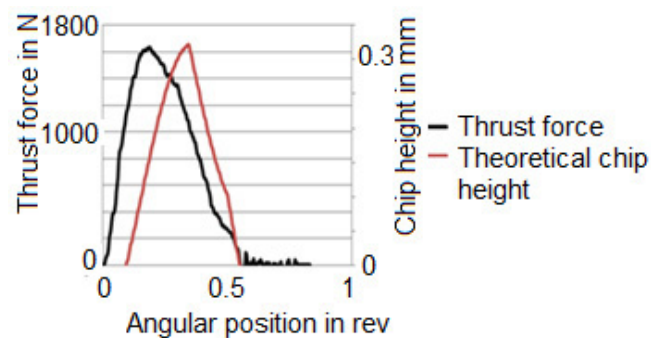


Fig. 11. Comparison of experimental thrust forces and theoretical chip height for $f = 0.2 \text{ mm}\cdot\text{rev}^{-1}$ and $a = 0.5 \text{ mm}$.

Moreover, it was observed that the maximal thrust force measured (Fig. 8A) appeared before the maximal theoretical chip height, which corresponds to the maximal thrust force calculated by the power model (Fig. 8B). Therefore, the maximal thrust force measured does not correspond to the maximal chip height. It is supposed that the instantaneous feed rate has an important influence on the thrust force generated. This influence of the instantaneous feed rate is not considered in the power model, but it is taken into account in the model suggested. The thrust force is increased when the tool goes down with important instantaneous feed rates. As the tool goes upward, the thrust force is reduced. By this way, the instant of maximum thrust force is better simulated by the suggested model.

Concerning the simulation of the maximal thrust force, the power model offers variable results. It is overestimated at low amplitudes and underestimated at high amplitudes. Despite its ability to represent and to explain the shape of the experimental thrust force, the model suggested underestimates the maximal thrust force for any amplitude.

From these observations, the relevance of the suggested model over a power regression model to represent the thrust force in vibration assisted drilling is pointed out. The main advantage of the model presented is its ability to define the evolution of the thrust force, which is completely different from the evolution of the chip height.

The drawback of the model remains in the determination of the chip height through the study of the kinematics

of vibration assisted drilling. As it can be seen in Figures 12 and 13, cutting time is underestimated by the kinematic model in all cases of interrupted cutting. The measured thrust force can be important while the simulated thrust force is null, corresponding to a theoretical chip height equal to zero (Fig. 11).

This may be explained by a reduction of the amplitude set while cutting. To confirm this hypothesis and the kinematic model, it would be best to measure the axial position at the tip of the tool. However, it is difficult to measure the tool trajectories because of the cutting zone being confined in drilling. The kinematics was observed indirectly by analysing its effects on several phenomena.

4.2 Kinematic model

The first point observed is the state of chips for several couples of feed-amplitude. In the first part, the definition of the amplitude limit of chip fragmentation was presented. In a feed versus amplitude plot, this limit is a theoretical straight line. From experimental tests, observation of the shape of the chip (continuous or fragmented) in relation to the cutting conditions, allows to define the experimental limit of fragmentation.

The results of experiments (Fig. 12) show that the amplitude set on the vibratory system to obtain fragmentation is approximately twice the theoretical amplitude. It guides toward the consideration of a reduction of the

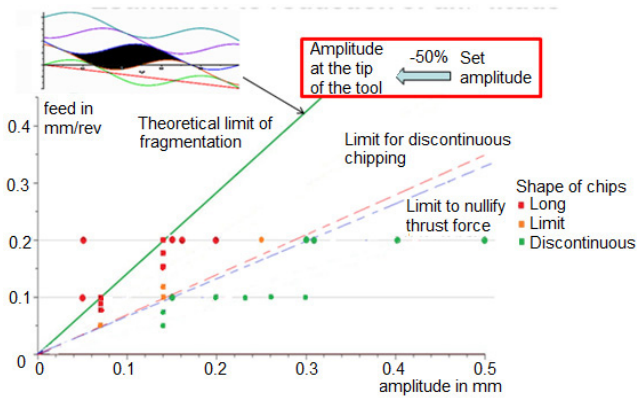


Fig. 12. Underestimated amplitude for chip fragmentation.

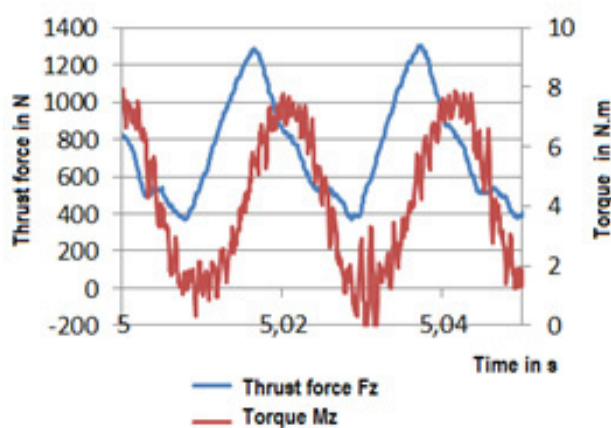


Fig. 13. Signal of thrust force and torque for $f = 0.2 \text{ mm} \cdot \text{tr}^{-1}$ and $a = 0.3 \text{ mm}$, chips are fragmented.

amplitude of oscillations during the cutting operation estimated at 50%.

It is supposed that this reduction of amplitude is caused by flexibility in the kinematic chain. This flexibility should be mainly present in the mechanical system generating the oscillations. Flexibility on the machining fixture may also reduce the amplitude of the oscillations.

During those tests, it was also observed some cases where the chip is fragmented but the thrust force does not come back to zero (Fig. 13). A second limit, for which the thrust force comes to zero, can be defined. However, the torque measured does come back to zero for those cases where the amplitude is close to the limit of chip fragmentation.

It was supposed that a phenomenon specific to vibration assisted drilling is involved. It generates large thrust force when generating negligible torque. Therefore, this phenomenon should happen at the centre of the tool. To highlight it, tests were conducted by drilling rods and drilling with pilot holes with vibration assistance. They permit respectively to consider mainly the cutting phenomena at the centre of the tool or excluding them from the analysis.

For these tests, rods and pilots holes of specific diameters are prepared to be drilled with the help of vibrations.

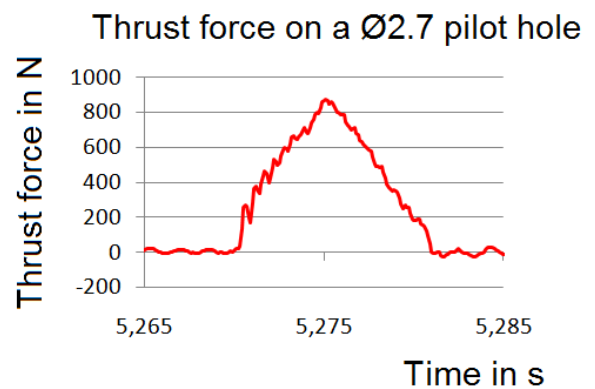
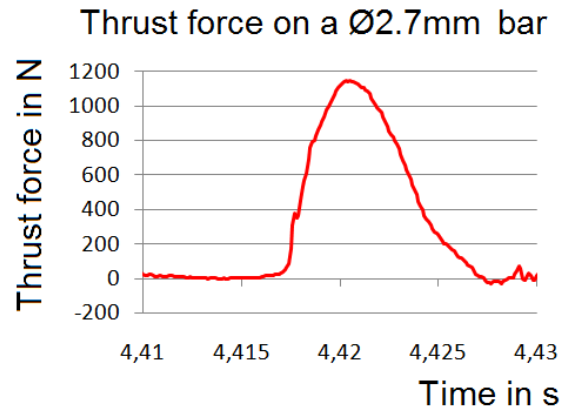


Fig. 14. Thrust force measured on a rod and a pilot hole for $a = 0.5 \text{ mm}$.

After simulating the radii of the indentation and intermediary zones, $\text{Ø}2.7 \text{ mm}$ and $\text{Ø}4.14 \text{ mm}$ are chosen. Figure 14 shows the thrust force signals obtained on a rod and a pilot hole for the maximal amplitude of 0.5 mm .

At the centre of the tool, when drilling rods, the thrust force has a fast increase at entry of the tool. Then, the thrust force decreases when the chip height still increases. The thrust force at the centre of the tool is highly related to the instantaneous feed rate.

On the cutting edges, when drilling pilot holes, the evolution of the thrust force has the same evolution as the chip height. The cutting speed is from 2, at the beginning of the cutting edge, to 25 times, at the corner of the tool, more important than the maximal instantaneous feed rate. The oscillations of the feed rate do not have as significant influence as for the indentation and intermediary zones.

The tool has a radius of 6.35 mm . Those results also show that the centre of the tool, with a radius of 1.35 mm , generates as much thrust force as the remaining area with a 5 mm radius. For a radius of 2.07 mm , the centre of the tool generates twice as much force as the remaining area.

It was proceeded to add the thrust force measured on a rod and on the pilot hole of the same diameter, expecting to retrieve the total thrust force in full cut for the same cutting conditions (Fig. 15). The results of the sum are

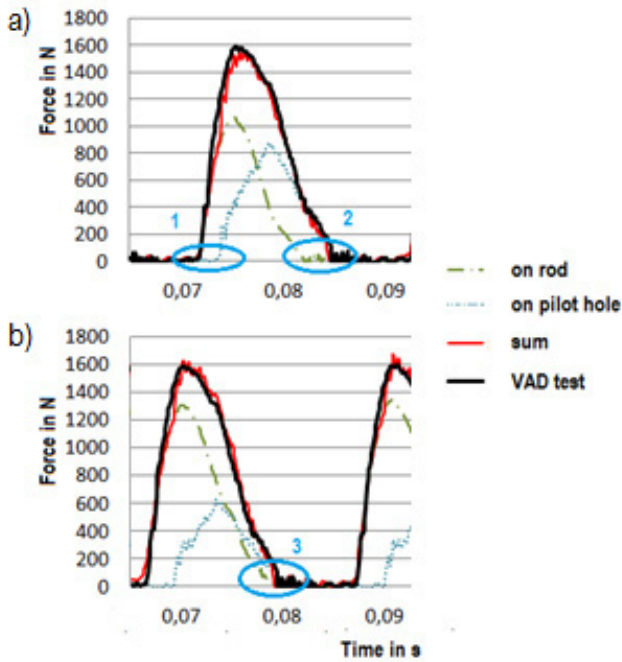


Fig. 15. Sum of thrust forces measured on rods and pilot holes for $a = 0.5$ mm of diameters (a) $\text{Ø}2.7$ and (b) $\text{Ø}4.14$.

quite precise as long as the two signals are synchronized to approach the thrust force in full cut.

A few points, represented on the graphs, can be brought to attention:

1. The center of the tool comes into contact ahead of time in comparison to the cutting edges. This may be explained by interference phenomena at the center of the tool. Interference phenomena are similar to indentation in the way that it represents a body penetrating another.
The kinematic model used to calculate the chip height simulates the movement of the cutting edges. Therefore, it does not take into account the tool geometry with its flank face and rake face at the center of the tool. It is then difficult to foresee the interferences of those faces penetrating the pushed material and generating interferences. Moreover, the material is not cut but pushed and plastically deformed because of the low cutting velocity, making it difficult to be simulated.
2. It is shown here that the center of the tool is not in contact when the tool goes upward. The center of the tool is exiting the material ahead of time on each oscillation in the case of interrupted cutting.
3. In the case of a radius of 2.07 mm, the mechanisms encountered on the rod are both indentation and cutting mechanisms. The cutting time is complete as the interference phenomenon starts earlier and the cutting mechanism ends later.

The maximal thrust forces on rods and pilot holes are not synchronized. The thrust force at the center of the tool is increased by the important feed rates at the beginning of

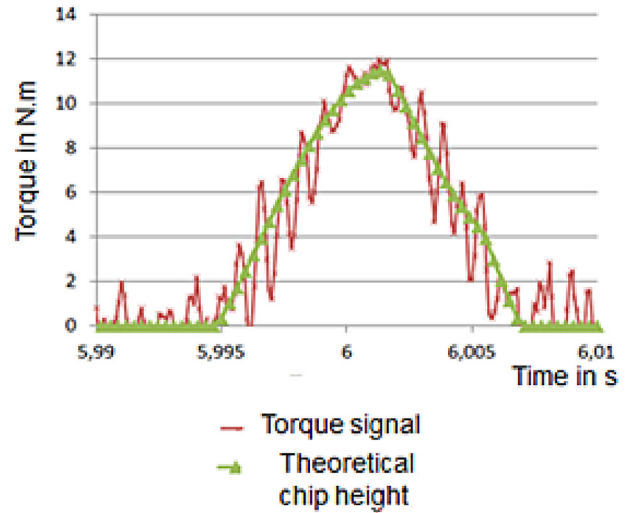


Fig. 16. Comparison of measured torque with theoretical chip height for $f = 0.2 \text{ mm}\cdot\text{rev}^{-1}$ and $a = 0.5$ mm.

each cut. The thrust force on the cutting edges depends on the chip height. The maximal thrust force in full cut is closer to the moment the thrust force at the center of the tool is at its peak.

From these observations, the presence of interferences at the centre of the tool may explain why the cutting time on thrust force signal is still underestimated by the kinematic model, even if a reduced amplitude is considered. The centre of the tool generates a thrust force before the cutting edges, but does not generate much torque. Therefore the cutting time observed on torque signals corresponds better to the simulated one. The fragmentation limit observed on chips does relate to the cases where the torque reaches zero.

Because the material is not cut but plastically deformed and pushed in this zone, it is difficult to estimate the size of the area concerned by interference phenomena. When compared to indentation phenomenon, it can be supposed that its size approaches a few tenths of millimetres. The authors suggest finite elements method or using high-speed camera when drilling to further study the interferences happening at the centre of the tool.

4.3 Torque model

Because the presence of interferences at the centre of the tool does not generate much torque, they can be neglected when modelling it. Considering the reduction of amplitude, a torque model is suggested. Figure 16 shows a signal of the torque measured in vibration assisted drilling with a feed $f = 0.2 \text{ mm}\cdot\text{rev}^{-1}$ and an amplitude $a = 0.5$ mm. It was observed that the torque had a quasi-linear relation with the chip height.

From this observation, a linear model of torque as a function of chip height is established from vibration assisted drilling data (Fig. 17).

$$M_z = K_{mz} D h_c \quad (11)$$

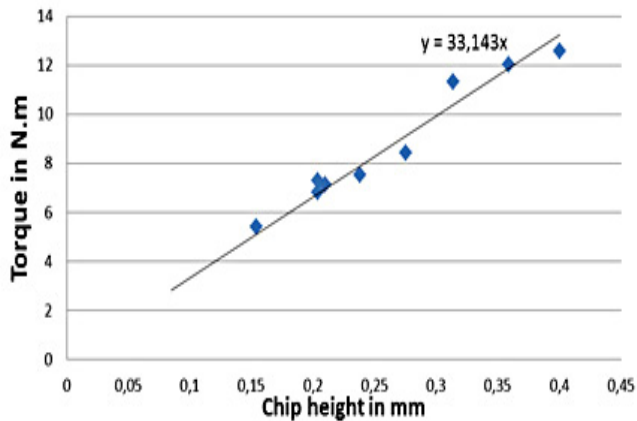


Fig. 17. Identification of the parameter K_{mz} of the torque model.

where D is the diameter of the tool and K_{mz} the parameter to identify.

From this identification, a value of 2.61 is obtained for the parameter K_{mz} , with a correlation coefficient of 0.96.

This model allows a good simulation of the torque generated during vibration assisted drilling. The modelling of the thrust forces is more difficult as it needs a better understanding of the interference phenomena.

5 Conclusions

In this paper, a kinematic model of vibration assisted drilling was developed. Chip height was simulated from the trajectories of the teeth of the tool. A divided model of the thrust force was proposed and applied to vibrations assisted drilling in aluminum. The following conclusions can be made:

- The divided model represents each zone of the tool with separate cutting mechanisms from the indentation phenomenon at the centre of the tool to the cutting mechanism on the cutting edges. Each zone has its size and the thrust force it generates related to instantaneous cutting conditions.
- The suggested model better simulates the evolution of the thrust force in vibration assisted drilling than a power model.
- The parameters of the suggested model are identified with traditional drilling data. This may explain the underestimation of the thrust forces.
- It is necessary to consider both the chip height and the instantaneous feed rate to model the thrust forces in vibration assisted drilling.
- Tests on rods and pilot holes show the different evolutions of the thrust force in relation to each cutting mechanism. The centre of the tool generates more thrust force with a smaller area because it is related to the instantaneous feed rate.

However, specific phenomena were highlighted in vibration assisted drilling, which modify the kinematics at the

tip of the tool and explain the differences observed on the thrust force model in regards to the experimental data. Results have shown that:

- The amplitude of oscillations is reduced during drilling. The reduction is estimated to 50%. It explains the need for a higher amplitude set on the vibratory system in order to fragment the chips.
- Interferences happen at the centre of the tool, increasing the cutting time observed on the thrust force signal. Those interferences cannot be simulated by a kinematic model because it is supposed to be due to a specific phenomenon at the centre of the tool.
- The torque signal can be used to identify the reduction of amplitude during drilling and the real limit of fragmentation.
- The torque was simulated as a linear function of the simulated chip height. The model is precise and its parameters can be identified with vibration assisted drilling data.

Future investigations need to be carried out to understand and model the interference phenomena at the centre of the tool. Furthermore, to avoid underestimation of the thrust force, a new methodology has to be developed to identify the divided model with vibration assisted drilling data instead of traditional drilling data.

Acknowledgements. This work was funded by the region Midi-Pyrenees and carried out within the context of the working group Manufacturing'21. It gathers 18 French research laboratories. The topics approached are the modelling of the manufacturing process, virtual machining and emerging manufacturing methods. We would also like to thank AIRBUS (Toulouse) and MITIS for providing the materials needed to carry out the study.

References

- [1] S. Tichkiewitch, G. Moraru, D. Brun-Picard, A. Gouskov, Self-Excited Vibration Drilling Models and Experiments, CIRP Annals – Manuf. Technol. 51 (2002) 311–314
- [2] H.G. Toews, W.D. Compton, S. Chandrasekar, A study of the influence of superimposed low-frequency modulation on the drilling process, Precision Eng. 22 (1998) 1–9
- [3] S. Laporte, C. De Castelbajac, Major Breakthrough in Multi Material Drilling, Using Low Frequency Axial Vibration Assistance, in: SAE Int. J. Mater. Manf. (2012) 1–12
- [4] J. Jallageas, Optimisation du perçage de multi-matériaux sur unité de perçage automatique (UPA), Thèse, Université de Bordeaux, 2013
- [5] S. Arul, The effect of vibratory drilling on hole quality in polymeric composites, Int. J. Mach. Tools Manuf. 46 (2006) 252–259
- [6] S. Chang, Burr height model for vibration assisted drilling of aluminum 6061-T6, Precision Eng. 34 (2010) 369–375
- [7] B. Pena, Monitoring of drilling for burr detection using spindle torque, Int. J. Mach. Tools Manuf. 45 (2005) 1614–1621

- [8] S. Basavarajappa, Drilling of hybrid metal matrix composites – Workpiece surface integrity, *Int. J. Mach. Tools Manuf.* 47 (2007) 92–96
- [9] C.C. Tsao, H. Hocheng, Evaluation of thrust force and surface roughness in drilling composite material using Taguchi analysis and neural network, *J. Mater. Process. Technol.* 203 (2008) 342–348
- [10] K. Palanikumar, Modelling and analysis for surface roughness in machining glass fibre reinforced plastics using response surface methodology, *Mater. Design* 28 (2007) 2611–2618
- [11] N. Guibert, Identification of thrust force models for vibratory drilling, *Int. J. Mach. Tools Manuf.* 49 (2009) 730–738
- [12] R.A. Williams, A study of the basic mechanics of the chisel edge of a twist drill, *Int. J. Prod. Res.* 8 (1970) 325–343
- [13] D. Bondarenko, Étude mésoscopique de l'interaction mécanique outil/pièce et contribution sur le comportement dynamique du système usinant, Thèse, Université de Bordeaux, 2011